AD NUMBER
AD037166
CLASSIFICATION CHANGES
TO: unclassified
FROM: confidential
LIMITATION CHANGES
TO: Approved for public release, distribution unlimited
FROM: Distribution authorized to U.S. Gov't. agencies and their contractors; Administrative/Operational Use; JAN 1954. Other requests shall be referred to U.S. Naval Ordnance Laboratory, White Oak, MD.
AUTHORITY
USNOL ltr, 25 Feb 1957; USNOL ltr, 29 Aug 1974

NOTICE: THIS DOCUMENT CONTAINS INFORMATION AFFECTING THE NATIONAL DEFENSE OF THE UNITED STATES WITHIN THE MEANING OF THE ESPIONAGE LAWS, TITLE 18, U.S.C., SECTIONS 793 and 794. THE TRANSMISSION OR THE REVELATION OF ITS CONTENTS IN ANY MANNER TO AN UNAUTHORIZED PERSON IS PROHIBITED BY LAW.

CONFIDENTIAL

NAVORD REPORT 3635

THE INFLUENCE OF CHAMBER DIAMETER ON THE MUZZLE VELOCITY OF A GUN WITH AN EFFECTIVELY INFINITE LENGTH CHAMBER

26 JANUARY 1954

U. S. NAVAL ORDNANCE LABORATORY
WHITE OAK, MARYLAND

CONFIDENTIAL

NAVORD Report 3635

Aeroballistic Research Report 218

THE INFLUENCE OF CHAMBER DIAMETER ON THE MUZZLE VELOCITY OF A GUN WITH AN EFFECTIVELY INFINITE LENGTH CHAMBER

Prepared by:

Arnold E. Seigel

ABSTRACT: This report is a theoretical study of the influence of chambrage (the ratio of chamber diameter to bore diameter) on the muzzle velocity of a gun. The analysis is applied to a chambered gun in which all the propellant is burned before the projectile moves; the cylindrical chamber is assumed to be of sufficient length so that the breech has no effect on the projectile motion. Thus, the influence of chambrage is present, while the effects of the propellant burning during firing and of the breech are not. The propellant gas is treated as an ideal gas. The change of state of the gas in passing through the section of reduction in diameter is obtained by applying the steady state isentropic equations of continuity and energy. Unsteady isentropic flow is assumed in all other parts of the gun. [illegible] sle velocity as a function of chambrage are obtained.

U. S. NAVAL ORDNANCE LABORATORY
WHITE OAK, MARYLAND

NAVORD Report 3635

26 January 1954

This report presents further results of a theoretical study of the effect of gun chambrage (the ratio of propellant chamber diameter to barrel bore diameter) on the muzzle velocity of guns. It considers the effect of finite chambrage and is a sequel to NAVORD Report 2691, which treats the special case of infinite chambrage. This study was made in order to augment our interior ballistics knowledge with the ultimate aim of obtaining high gun velocities. The work was carried out under project No. FR-33-(54).

EDWARD [illegible] WOODYARD
Captain, USN
Commander

M. H. KURZWEG, Chief
Aeroballistic Research Department
By direction

CONTENTS

ILLUSTRATIONS

THE INFLUENCE OF CHAMBER DIAMETER ON THE MUZZLE VELOCITY OF A GUN WITH AN EFFECTIVELY INFINITE LENGTH CHAMBER

I. INTRODUCTION

1. The influence of chambrage, the ratio of the propellant chamber diameter to the barrel bore diameter, has been theoretically examined in reference (a) for the special case known as "optimum chambrage". This condition of chambrage equal to infinity yields the maximum possible projectile velocity for given gun and propellant parameters.* (In most instances the optimum chambrage conditions can be approached by either a large, well-shaped chamber in which the propellant has been initially all burned or by a propellant burning at the proper rate in a smaller chamber (see reference (a).) It is of interest here to determine quantitatively the effect of finite chambrage on the muzzle velocity of guns.

2. In reference (a) a qualitative description of what occurs during the firing of a conventional chambered gun is given in terms of the rarefactions and compression impulses which are present in the propellant gas. It is demonstrated that the propellant gas directly behind the projectile experiences chiefly the following tendencies for changes in pressure:

a. A drop in pressure from the rarefactions [illegible] accelerating projectile

b. A rise in pressure from the compressions produced by the burning propellant

c. A drop in pressure caused by the rarefactions reflected from the breech

d. As a result of chambrage, a rise in pressure from the compressions reflected from the transition section, which joins the chamber to the barrel.

A study will be made here of a gun with finite chambrage in which the propellant is initially all burned and which has a sufficiently long chamber so that the breech has no effect on the projectile motion. In this simplified gun the effects of the burning propellant and of the breech, (b) and (c) above, are absent; and the influence of chambrage on the accelerating projectile, (a) and (d) above, can therefore be obtained apart from these effects.

---

* The propellant is assumed to burn only in the chamber.

3. The one-dimensional characteristic equations are applicable to the chamber (considered to be of constant diameter) and to the constant diameter barrel:

$$\frac{\partial}{\partial t}(u \pm \sigma) + (u \pm a)\frac{\partial}{\partial x}(u \pm \sigma) = 0 \quad (1)$$

*

In general, the solution of these equations requires a numerical step-by-step procedure for both the chamber and the barrel sections; this procedure can be applied to any length chamber and barrel. In the particular case analyzed here of a long (effectively infinite length) chamber in which the propellant is initially all burned, the equation with positive signs of equation (1) integrates simply into

$$u + \sigma = \sigma_0 \quad (2)$$

**

for the chamber section; consequently, no step-by-step procedure is required in this case for the chamber section. (An effectively infinite length chamber is one sufficiently long so that no impulses or disturbances reflected from the chamber back end reach the projectile. See Section VI for a quantitative determination of this necessary length.)

4. The gas flow in the transition section, which joins the chamber to the bore, can be described by the two-dimensional unsteady adiabatic energy equation and the two-dimensional unsteady continuity equation. Since it is not feasible to use these equations, it is assumed that the rate at which the gas passes through the transition section is large relative to the rate at which conditions change within the transition section. Then the equations which are applicable to relate the conditions in a particular gas layer at the entrance of the transition section to those in this same gas layer when it is at the exit of the transition section are the steady equations of continuity and energy. By steady equations is meant that the equations

$$\rho u A = \text{constant} \quad (3)$$

$$\text{and } \frac{u^2}{2} + h = \text{constant} \quad (4)$$

are applied to each gas layer, the constants in general being slightly different for each successive layer.

5. It can be shown by the same arguments as presented in reference (a) that the use of the steady flow equations to describe the gas flow between the chamber and the barrel of a gun yields a larger projectile velocity than the use of the unsteady equations. (The accuracy of the

---

* See List of Symbols.

** This is true because all downstream characteristic lines in the chamber originate from gas at rest and at the initial thermodynamic state of the gas. For a detailed explanation, see reference (d).

steady flow approximation to the unsteady condition can be obtained from specific gun experimental results.*) In support of the use of this approximation, however, is the realization that the steady state condition is approached in the transition section of our simplified gun with the passage of time.

6. With the assumptions stated above and the additional assumption that the process is thermodynamically reversible, it is possible to study quantitatively the influence of chamber diameter on the muzzle velocity of guns. The method of calculation and the results obtained are presented below.

II. Equations Describing the Behavior of the Propellant Gas and the Projectile

7. The gun is visualized as having a constant-diameter chamber of effectively infinite length joined by a transition section to a constant-diameter barrel. The projectile is positioned initially so that its back end is at the beginning of the uniform-area barrel section. It is assumed that the propellant burns completely before the projectile begins to move, producing the high-pressure propellant gas at initial and peak pressure p_o and sound velocity a_o (see sketch below).

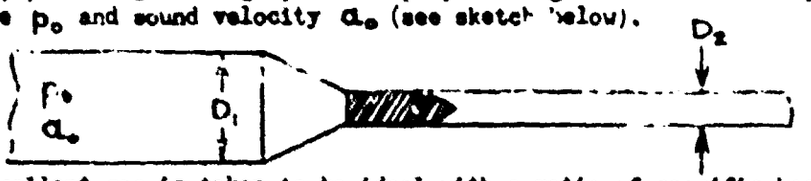

The propellant gas is taken to be ideal with a ratio of specific heats, γ, of 1.4. (The method used, however, can be applied to an imperfect gas or an ideal gas of any γ (see reference (d)). The value of 1.4 is selected because experiments to confirm the theoretical conclusions obtained in this report were carried out using air; these experiments are described in reference (b). For generality, dimensionless variables are used; these are listed below:

$$\bar{x} = \frac{p_o A x}{M[2/(\gamma-1)]^2 a_o^2} = \frac{p_o A x}{25\, a_o^2 M}$$

$$\bar{t} = \frac{p_o A t}{M[2/(\gamma-1)] a_o} = \frac{p_o A t}{5\, a_o M}$$

* Such experimental results are described in reference (b).

$$\bar{u} = \frac{u}{[2/(\gamma-1)]a_0} = \frac{u}{5\,a_0}$$

$$\bar{a} = \frac{a}{[2/(\gamma-1)]a_0} = \frac{a}{5\,a_0} \qquad (5)$$

$$\bar{p} = \frac{p}{p_0}\,, \quad \bar{\rho} = \frac{\rho}{\rho_0}\,, \quad \bar{\sigma} = \frac{\sigma}{\sigma_0}$$

8. It is assumed that each part of the propellant gas expands isentropically; therefore, since the propellant gas is ideal,

$$\bar{p} = \bar{\rho}^{\gamma} = \bar{\rho}^{1.4}, \quad \sigma = \int_0^{\rho} a\, d\rho/\rho = 2a/(\gamma-1)$$

$$\bar{\sigma} = 2\bar{a}/(\gamma-1) = 5\bar{a}, \quad \bar{p} = \bar{\sigma}^{2\gamma/(\gamma-1)} = \bar{\sigma}^{7} \qquad (6)$$

Further, in the uniform chamber section and in the uniform barrel section the assumption is made that the gas motion is once dimensional in space. From this assumption and that of isentropicity, the unsteady one-dimensional momentum equation and continuity equation lead to the one-dimensional characteristic equations. Written in dimensionless form, these equations are

$$\frac{\partial}{\partial t}(\bar{u} \pm \bar{\sigma}) + (\bar{u} \pm \bar{a})\frac{\partial}{\partial x}(\bar{u} \pm \bar{\sigma}) = 0 \qquad (7)$$

Equations (7) apply to both the chamber and barrel sections. Since the chamber is effectively infinite in length (and, consequently, the back part of the propellant gas remains at rest in its initial state in the charber), the equation with positive signs of equation (7) becomes

$$\bar{u} + \bar{\sigma} = 1 \qquad (8)$$

Thus, for the chamber section the sum of the gas velocity, $\bar{u}$, and the Riemann function, $\bar{\sigma}$ (equal to $2/(\gamma-1)$ times the sound velocity), remains a constant. This fact simplifies the treatment of the propellant gas in the chamber section. In the barrel section, however, no such simplification is possible; and equations (7) must be solved by a numerical step-by-step process.

9. In the transition section, which joins the chamber of cross-sectional area A_1 to the barrel of cross sectional area A_2, the gas flow is described by the steady flow equations of continuity and energy. With the subscript "1" denoting the state of the gas in the chamber at the entrance to the transition section, and the subscript "2" denoting the state of the gas in the barrel at the exit of the transition section (see sketch), these equations are:

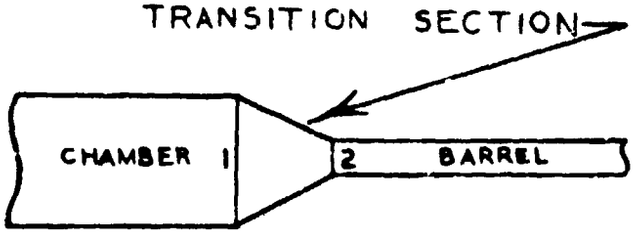

$$\rho_1 u_1 A_1 = \rho_2 u_2 A_2$$

$$\text{and} \quad h_1 + u_1^2/2 = h_2 + u_2^2/2 \tag{9}$$

In dimensionless form equations (9) become, with the use of equations (5) and (6),

$$\left(\bar{\sigma}_1\right)^{\frac{2}{\gamma-1}} \bar{u}_1 \frac{A_1}{A_2} = \left(\bar{\sigma}_2\right)^{\frac{2}{\gamma-1}} \bar{u}_2 \tag{10}$$

$$\text{and} \quad \bar{u}_1^2 + \frac{\gamma-1}{2}\bar{\sigma}_1^2 = \bar{u}_2^2 + \frac{\gamma-1}{2}\bar{\sigma}_2^2 \tag{11}$$

where the enthalpy h has been replaced by its equivalent for the ideal gas, $(\gamma-1)c^2/\gamma$.

10. Equation (8) can be applied in particular to the entrance of the transition section, yielding

$$\bar{u}_1 + \bar{\sigma}_1 = 1 \tag{12}$$

With the assumption that the projectile is unopposed by air pressure in front and friction forces, the equation for the projectile acceleration is

$$\frac{d\bar{u}}{dt} = \bar{p} \tag{13}$$

From equations (7), (10), (11), and (13) the entire behavior of the gas and projectile can be obtained for the chambered gun with effectively infinite length chamber.

III. Obtaining Maximum Projectile Velocity for the Chambered Gun

11. By the use of the equations presented in Section II, the maximum projectile velocity can be obtained easily as a function of the ratio of chamber diameter to barrel diameter. The maximum projectile velocity is attained by an unopposed projectile in a gun of infinite barrel length. Although this velocity is an idealized limit, it is instructive to see the effect of chambrage on this limit.

12. As the projectile velocity increases in a chambered gun with infinite chamber length and infinite barrel length, steady state conditions in the transition section are approached, and the velocity at the exit of the transition section approaches the local sonic velocity.* When the projectile has reached its maximum velocity, the steady state conditions will exist in the transition section, and the gas will be flowing with sonic speed. Thus, the steady flow equations (10) and (11) will exactly apply at this time; and, in addition, the velocity at the transition section exit can be equated to the sonic velocity without approximation.

$$(\bar{\sigma}_1)^{\frac{2}{\gamma-1}}\,\bar{u}_1\,\frac{A_1}{A_2} = (\bar{\sigma}_2)^{\frac{2}{\gamma-1}}\,\bar{u}_2 \qquad (10)$$

$$\bar{u}_1^2 + \frac{\gamma-1}{2}\bar{\sigma}_1^2 = \bar{u}_2^2 + \frac{\gamma-1}{2}\bar{\sigma}_2^2 \qquad (11)$$

$$\bar{u}_2 = a_2 = \frac{\gamma-1}{2}\,\bar{\sigma}_2 \qquad (14)$$

where all the quantities are for the time when the projectile velocity is a maximum.

13. As the chamber is effectively infinite in length, equation (8) can be applied to the gas in the chamber at the entrance to the transition section at this time

$$\bar{u}_1 + \bar{\sigma}_1 = 1 \qquad (12)$$

To determine the maximum projectile velocity, the impulses traveling downstream from the transition section toward the projectile may be examined. For each of these impulses the quantity $\bar{u} + \bar{\sigma}$ is a constant (by equation (7)), a different constant for each impulse, equal to $\bar{u}_2 + \bar{\sigma}_2$, since they travel from the exit of the transition section. When the projectile is traveling at maximum speed, the pressure of the gas directly behind it is zero, and hence the Riemann function $\bar{\sigma}$ of

---

* The maximum velocity with which gas can issue from the chamber into the barrel is the local velocity of sound; this is true whether the flow is steady or unsteady.

this gas (by equation (6)) is zero. Therefore,

$$\bar{u}_M = (\bar{u} + \bar{\sigma})_{AT\ PROJ.} = \bar{u}_2 + \bar{\sigma}_2 \quad (15)$$

where $\bar{u}_M$ is the dimensionless maximum projectile velocity, and the quantities in the equation refer to the time when the projectile velocity is a maximum. With equation (14) the maximum projectile velocity becomes

$$\bar{u}_M = \frac{\gamma+1}{\gamma-1}\bar{a}_2 = \frac{\gamma+1}{2}\bar{\sigma}_2 \quad (16)$$

14. From equations (10), (11), (12), (14), and (16) the relation between the maximum projectile velocity and the ratio of the chamber-to-bore cross-sectional area (or chamber-to-bore diameter) can be obtained for the infinite-chamber-length gun. $A_1/A_2 = (D_1/D_2)^2 =$

$$= \left[\frac{\bar{u}_M}{1 + \sqrt{\left(\frac{\gamma-1}{2}\right)\left(\bar{u}_M^2 - 1\right)}}\right]^{\frac{2}{\gamma-1}} \left[\frac{\bar{u}_M}{1 - \frac{2}{\gamma-1}\sqrt{\left(\frac{\gamma-1}{2}\right)\left(\bar{u}_M^2 - 1\right)}}\right] \quad (17)$$

It is evident from equation (17) that, as expected, the maximum projectile velocity for an infinite-chamber-length, constant-diameter gun ($D_1/D_2 = 1$) is $2a_o/(\gamma-1)$ (i.e., $\bar{u}_M$ is equal to 1). Further, it is seen that as D_1/D_2 approaches an infinite value — this would be the case of the optimum chambrage gun — $\bar{u}_M$ approaches the value $\sqrt{(\gamma+1)/2}$ (or u_M approaches $\left(\sqrt{(\gamma+1)/2}\right) 2a_o/(\gamma-1)$); this result agrees with the maximum velocity result obtained in reference (a) for the optimum chambrage gun.

15. For a propellant gas of γ equal to 1.4, the maximum projectile velocity has been evaluated as a function of D_1/D_2 from equation (17). The result is shown in Figure 1.

16. The increase in the maximum projectile velocity as a result of chambrage divided by the increase in the projectile velocity as a result of optimum chambrage, expressed as a percentage, is designated the percent of the optimum chambrage maximum velocity increase. Thus, percent of the optimum chambrage maximum velocity increase

$$= \frac{u_M - 2a_o/(\gamma-1)}{\left(\sqrt{2/(\gamma+1)}\right) 2a_o/(\gamma-1) - 2a_o/(\gamma-1)} \quad (18)$$

$$= \frac{\bar{u}_M - 1}{\sqrt{2/(\gamma+1)} - 1}$$

This percentage has been calculated as a function of chamber-to-bore diameter (D_1/D_2) for both a γ equal to 1.4 propellant gas and a γ equal to 1.25 propellant gas. The results are presented in Figure 2 as a single curve, because, quite surprisingly, the percentage was

found to be almost exactly the same for each γ ; this demonstrated that the percentage of the optimum chambrage maximum velocity increase is practically independent of γ between the limits of γ equal to 1.25 to 1.4.

17. It might be reiterated at this point that the equations used in obtaining Figures 1 and 2 are not approximate ones but exactly describe the assumed isentropic gas flow for an infinite-chamber-length gun when the projectile velocity is a maximum.

IV. Method of Calculation of the Projectile Velocity for a Chambered Gun

18. To calculate the projectile velocity for a chambered gun of effectively infinite length from equations (7), (10), (11), and (13), it is necessary to use in the barrel section the step-by-step numerical characteristics method. (This method is outlined in references (b), (c) and (f), and in many other reports.) This requires the use of a characteristics net (two sets of intersecting characteristic lines in the x - t plane -- one with slope $\bar{u} + \bar{a}$, along which $\bar{u} + \bar{\sigma}$ is constant, another with slope $\bar{u} - \bar{a}$, along which $\bar{u} - \bar{\sigma}$ is constant). The characteristic lines forming the net can be interpreted as the path of disturbance impulses, since, as one goes along a characteristic line, one travels at the same speed as a disturbance would, that is, at the local velocity of sound relative to the moving gas.

19. A schematic drawing of a characteristics diagram for a chambered gun is shown in Figure 3. In this figure the points O, A, B, C, D, etc. are points on the projectile path; the line O-O' represents the beginning of the constant-diameter barrel section, the line T-T' represents the end of the constant-diameter chamber section.

20. For the calculation the relationship between conditions at the entrance and exit to the transition section is obtained from equations (10), (11), and (12). Thus, these equations can be combined to yield the relation between $\bar{\sigma}_1$ and $\bar{\sigma}_2$,

$$\frac{1}{\bar{\sigma}_1} = \left| + \left\{ \frac{1 - (\bar{\sigma}_2/\bar{\sigma}_1)^2}{[2/(\gamma-1)]\left[(\bar{\sigma}_1/\bar{\sigma}_2)^{4/(\gamma-1)}(A_1/A_2)^2 - 1\right]} \right\}^{\frac{1}{2}} \right. \tag{19}$$

With equation (19), equations (10) and (12) conveniently yield the relations between $\bar{\sigma}_1$, $\bar{\sigma}_2$, $\bar{u}_1$ and $\bar{u}_2$ for use in the calculation.

21. To begin the numerical solution, an initial point along the projectile path (point A in Figure 3) can be obtained by assuming that the pressure-velocity relationship behind the projectile up to that point

is the same as that at the exit of the transition section. This approximation has been found to be satisfactory up to $\bar{u} = .08$ for the optimum chambrage gun; it can be made as accurate as desired by taking point A as close as desired to point O.

22. The characteristics net is continued from point A by the usual numerical methods. Thus, from points O and A, point 1 is calculated; from 1 and A, point B is calculated, and so on. Conditions at the exit of the transition section (represented by points 1, 2, 3, 4, etc.) are calculated from the value of $\bar{u} - \bar{\sigma}$ on the upstream impulses (e.g., A-1, B-2, C-3, etc.) and the use of equations (19), (10), and (12). To prevent the characteristics net from becoming too coarse, a parabola is fitted through the points D, E, and F in Figure 3. With this parabola the points α, β, γ, ξ, δ, and ζ are calculated and used to continue the characteristics net.

V. Calculated Projectile Behavior for a Gun with Chamber-to-Bore Diameter Ratio Equal to 1.5

23. From the relation between the maximum velocity and the chamber-to-bore diameter ratio, equation (17), and the expression for the percent velocity increase, equation (18), the diameter ratio which yields a value of 50% of the optimum chambrage maximum velocity increase can be calculated. This diameter ratio D_1/D_2, is equal to 1.511 for a γ equal to 1.4 propellant gas (and approximately equal to the value for a γ equal to 1.25 gas (see Figure 2)); therefore, the calculation of projectile behavior was done for a chambered gun with D_1/D_2 equal to 1.511. A portion of the actual characteristics diagram is shown in Figure 4. The calculated values for points along the projectile path of the $D_1/D_2 = 1.511$ gun are given in Table I (1.511 is often denoted 1.5).

24. Plots of projectile velocity $\bar{u}$ versus travel $\bar{X}$ are given in Figure 5 for guns using a $\gamma = 1.4$ gas, with chamber-to-bore diameter equal to 1 (see reference (a)), 1.511 (the case calculated here), and ∞ (optimum chambrage gun). (Figure 6 is the $\bar{u}$ versus $\bar{X}$ plot in the lower velocity region.) It is apparent from these curves that the velocity of the $D_1/D_2 = 1.511$ gun is approximately halfway between the $D_1/D_2 = 1$ and the $D_1/D_2 = \infty$ gun velocities. Thus, the $D_1/D_2 = 1.5$ gun, which yields 50% of the optimum chambrage velocity increase at maximum velocity, is seen to yield approximately 50% of the optimum chambrage velocity increase for all velocities. The curve of Figure 2, which applies to the maximum velocity increase at infinite travel, therefore, can be applied to the velocity increase of a chambered gun at any projectile travel. This curve is replotted in Figure 7 with the ordinate labeled the "percent of the optimum chambrage velocity increase",

$$\frac{u \quad \text{---} u_{D_1/D_2 = 1}}{u_{D_1/D_2 = \infty} - u_{D_1/D_2 = 1}}$$

where u is the projectile velocity of the chambered gun, $u_{D_1/D_2=1}$ is the projectile velocity of the constant-diameter gun, and $u_{D_1/D_2=\infty}$ is the projectile velocity of the optimum chambrage gun, all to be taken at a given projectile travel. Figure 8 is a $\bar{u}$ versus $\bar{x}$ plot for chambered guns (D_1/D_2 = 1, 1.5, ∞) drawn for γ equal to 1.25 by analogy with the γ equal to 1.4 plots.*

25. Figures 5, 6 (or 8), and 7 can now be employed to obtain the projectile velocity for any chambered gun with effectively infinite length chamber. For example, to obtain the muzzle velocity of an effectively infinite chamber length gun of D_1/D_2 = 2, and γ = 1.4, whose dimensionless barrel length $\bar{x}$ equals .015, one would find from Figure 7 that the optimum chambrage velocity increase is 70 percent. From Figure 6, $\bar{u}_{D_1/D_2=1}$ = .126, $\bar{u}_{D_1/D_2=\infty}$ .149; therefore

$$\frac{\bar{u} - .126}{.149 - .126} = .70$$

and the velocity of this gun would be

$$\bar{u} = .142, \quad \text{or} \quad u = .71\, a_o$$

VI. Calculation of the First Impulse Reflected from the Breech

26. It has been emphasized that the analysis presented in this paper is for a gun whose chamber length is effectively infinite. For a gun in which the propellant is initially all burned and motionless, the projectile behavior is unaffected by the chamber back end (the breech) until the rarefaction impulses which originate from the projectile motion are reflected from the breech and reach the projectile. (The first such impulse is referred to as the first reflected impulse from the breech.) A gun whose chamber length is effectively infinite is, therefore, one in which the chamber is of sufficient length so that the first reflected impulse does not reach the projectile while it is in the barrel. A gun whose barrel length is short would require a relatively short chamber for an effectively infinite chamber length, whereas a long barreled gun would require a relatively long chamber. The impulses reflected from the breech which originated from the projectile are rarefaction impulses; when they reach the projectile, they lower the pressure of the gas behind the projectile, and, consequently, the projectile velocity is less than if there were no breech reflecting these impulses. As the chamber-to-bore diameter ratio increases, the effects of these reflected

*An error in the γ = 1.25 case occurring in reference (a) has been corrected in Figure 8.

rarefaction impulses become less and less (see discussion in reference (a)). In fact, the one-dimensional theory used here demonstrates that if D_1/D_2 is infinite, there is no effect due to a breech.)

27. Obtaining the chamber length necessary to be effectively infinite requires the calculation of the path of the first reflected impulses. As before, the cases of $D_1/D_2 = 1$, 1.5, and ∞ are considered. For a gun of constant diameter, Heybey (reference (e)) has obtained analytic expressions for the path of the first reflected impulse in the case of a perfect gas. These may be transformed to yield

$$\overline{X}_{\infty} = \frac{(\gamma-1)^2}{2(\gamma+1)}\left[\frac{1}{(1-\overline{u}_{1st})^{(\gamma+1)/2(\gamma-1)}} - 1\right] \qquad (20)$$

where $\overline{X}_{\infty}$ is the dimensionless distance from the breech to the initial position of the projectile back end and $\overline{u}_{1st}$ is the dimensionless projectile velocity when the first reflected impulse reaches the projectile. The relation between the projectile velocity $\overline{u}$ and the travel $\overline{X}$ for a constant-diameter gun (reference (e)) is

$$\overline{X} = \frac{(\gamma-1)^2}{2(\gamma+1)}\left[\frac{2 - (\gamma+1)(1-\overline{u})}{(\gamma-1)(1-\overline{u})^{(\gamma+1)/(\gamma-1)}} + 1\right] \qquad (21)$$

From equations (20) and (21) the necessary chamber lengths, $\overline{X}_{\infty}$, to be effectively infinite can be obtained as functions of projectile travel (i.e., barrel length) and projectile velocity. These relations are shown in Figures 9 and 10 as the $D_1/D_2 = 1$ plots.

28. For simplicity in calculating the path of the first reflected impulse in the case of the chambered guns, the length of the transition section between the chamber and barrel is taken to be zero. An examination of equation (10) or (19) demonstrates that, for the optimum chambrage gun ($D_1/D_2 = \infty$), the velocity of the gas in the chamber section is zero, and the pressure, sound velocity, and other gas conditions in the chamber remain constant at their initial values. Thus, the impulses in the chamber section travel at the initial sound velocity; the time required for the first impulse to travel from the transition point and back is equal to $2X_{\infty}/a_0$ or, dimensionlessly, $4\overline{X}_{\infty}/(\gamma-1)$.

29. Each value of time (e.g., P in the sketch below) along the $\overline{X} = 0$ line (the beginning of the barrel) obtained from the optimum chambrage calculation can be taken to correspond to the time required for the first impulse to reflect from the breech to the transition section; the breech distance $\overline{X}_{\infty}$ is equal to $(\gamma-1)/4$ of this time, and the velocity, $\overline{u}_{1st}$, and position, $\overline{X}_{1st}$, of the projectile when the first impulse reaches it at Q can be obtained from the optimum chambrage calculation by following the downstream impulse from P. In this manner the paths of the first reflected impulses for the $D_1/D_2 = \infty$ case are

obtained. The resultant $D_1/D_2 = \infty$ plots are shown in Figures 9 and 10.

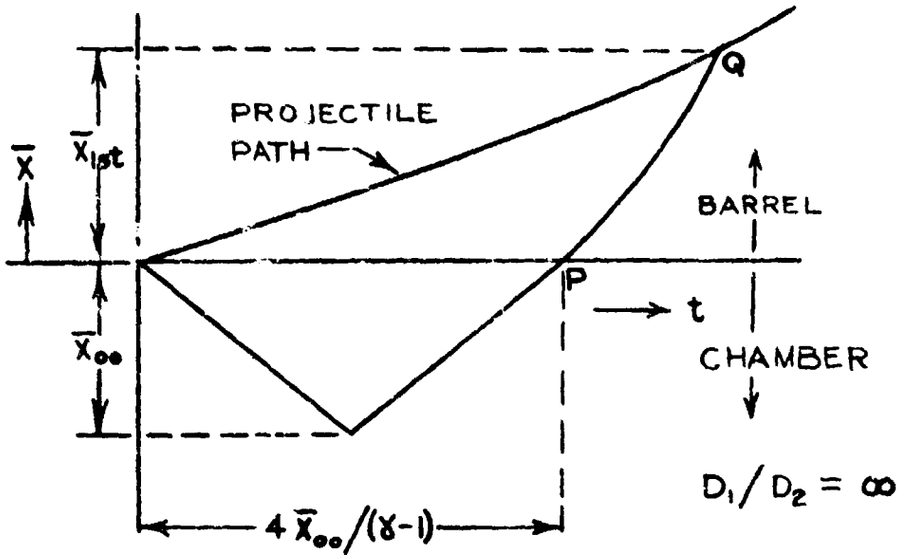

30. For the $D_1/D_2 = 1.5$ case the characteristic equations can be applied in the chamber section (where $\bar{u} + \bar{\sigma} = 1$) to obtain the path of the first reflected impulse. From points R and S used previously in the $D_1/D_2 = 1.5$ calculation, on the $\bar{X} = 0$ line (see sketch below) point T can be calculated; from T and U the point V can be calculated; etc.

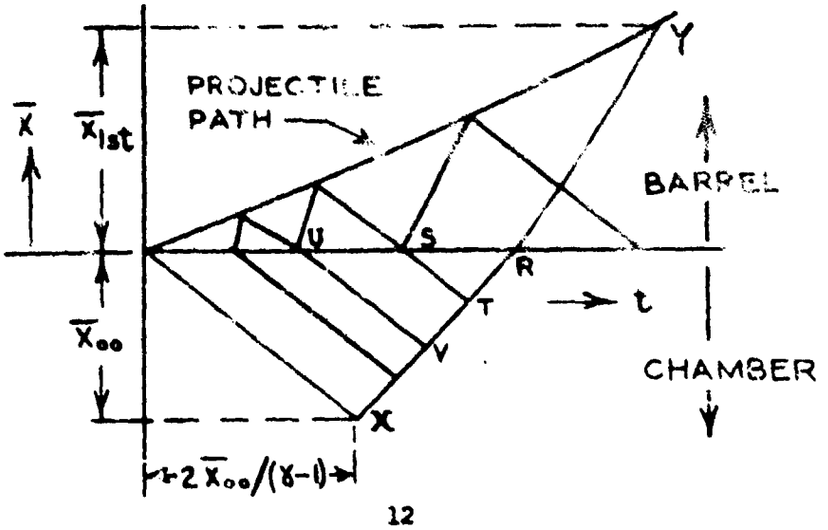

Point X, which specifies $\overline{X}_{\infty}$, is the intersection of the downstream characteristic R - T - V... and the first upstream impulse (of slope $-2/(\gamma-1)$). Since point Y on the projectile path has been calculated previously, the first reflected impulse path is completely known. In this manner the chamber length to be effectively infinite was calculated for the $D_1/D_2 = 1.5$ case; the results are shown in Figures 9 and 10.

31. The curves of Figures 9 and 10 illustrate that the $D_1/D_2 = 1.5$ case is approximately midway between the $D_1/D_2 = 1$ and $D_1/D_2 = \infty$ cases; therefore, the plot of Figure 2 (or 7) can be used to obtain the chamber lengths necessary to be effectively infinite for diameter ratios other than 1, 1.5, or ∞.

VII. CONCLUDING REMARKS

32. It is seen that the quantitative results obtained here are in agreement with the qualitative description of the effect of chambrage given in reference (a). There chambrage and a burning propellant are pictured as creating compression impulses which increase the projectile velocity. Alternately, chambrage and a burning propellant can be viewed as making possible the closer positioning of the propelling gas to the projectile, thereby increasing the projectile velocity.

33. It is to be emphasized that the conclusions obtained in this report on the influence of chambrage are applicable under the conditions that (a) the chamber and barrel are cylindrical, (b) the propellant gas is all burned before the projectile moves, (c) the propellant gas is an ideal gas, (d) the expansion of the gas is isentropic, (e) the chamber is sufficiently long that the breech has no effect on the projectile motion, and (f) the steady flow equations apply in the transition section. The validity of the last condition must await experimental results. The other conditions are not satisfied by conventional guns, and caution must be exercised in the application of these results to such guns; however, they are closely approached in some unorthodox guns to which these results can be directly applied. For conventional guns (i.e., in which the propellant burns during the projectile motion) the velocity gain from chambrage can be less than calculated here. This is due to the fact that a pressure sustaining effect behind the projectile can be achieved from the propellant's continued burning. This pressure sustaining effect from continued burning is more and more difficult to obtain as projectile velocities are increased (because of the high rates of burning required), but a pressure sustaining effect from chambrage is obtainable at high velocities. Thus, the use of chambrage is particularly advantageous in high-velocity conventional guns. NAVORD Report 3717 (in preparation) gives an approximate method of treating chambrage in conventional gun calculations.

TABLE I

POINTS ON THE PROJECTILE PATH
(Calculated for $D_1/D_2 = 1.5$, and $\gamma = 1.4$)

Point	$\bar{x}$	$\bar{t}$	$\bar{u}$	$\bar{\sigma}$	$\bar{p}$	$\bar{a}$
O	0	0	0	1.0	1.0	.20
A	.000482	.03167	.0300	.9845	.8965	.1969
B	.000687	.0376	.0353	.9792	.863	.1958
C	.001015	.0462	.0427	.9768	.849	.1954
D	.001660	.0597	.0538	.9683	.798	.1937
E	.003203	.0841	.0723	.9538	.718	.1908
α	.004029	.0951	.08	.9490	.694	.1898
β	.004639	.1026	.085	.9423	.660	.1885
γ	.005295	.1102	.090	.9378	.638	.1876
δ	.006018	.1181	.095	.9332	.616	.1866
ϵ	.006793	.1261	.100	.9289	.597	.1858
ζ	.007643	.1344	.105	.9248	.579	.1850
F	.008395	.1414	.1093	.9218	.565	.1844
G	.012491	.1744	.1268	.9074	.507	.1815
H	.015848	.2011	.1397	.8962	.464	.1792
I	.020333	.2317	.1533	.8851	.426	.1770
J	.026336	.2690	.1683	.8713	.381	.1743
K	.034034	.3127	.1840	.8569	.339	.1714
L	.044148	.3653	.2007	.8407	.297	.1681
M	.055197	.4184	.2156	.8265	.264	.1653
N	.158593	.8230	.2955	.7491	.131	.1498
O	.420088	1.6289	.3733	.6728	.062	.1346

LIST OF SYMBOLS

a - Velocity of sound

A_1 - Cross-sectional area of propellant chamber

A_2 - Cross-sectional area of barrel bore

D_1 - Diameter of propellant chamber

D_2 - Diameter of barrel bore

h - Enthalpy

M - Mass of projectile

p - Pressure

t - Time

u - Gas or projectile velocity

x - Position coordinate of gas element

x_{00} - Distance from breech to transition section

γ - Specific heat ratio

ρ - Gas density

σ - Riemann function, defined as $\int_0^{\rho} (a\, d\rho/\rho)_S$, S = entropy

A symbol with a bar is dimensionless and is related to the dimensional quantities by equations (5). The subscript "o" refers to the initial state of the gas at rest in the chamber; the subscript "1" denotes the state of the gas in the chamber at the entrance to the transition section, and the subscript "2" denotes the state of the gas in the barrel at the exit of the transition section.

REFERENCES

(a) NAVORD Report 2691, The Effect of the Optimum Chambrage on the Muzzle Velocity of Guns with a Qualitative Description of the Fundamental Phenomena Occurring During Gun Firing, by A. E. Seigel.

(b) NAVORD Report 3636, Results of Chambrage Experiments on Guns with Effectively Infinite Length Chambers, by A. E. Seigel and V. C. D. Dawson.

(c) P. Carrière, Proc. Seventh International Congress of Applied Mechanics 3, 139 (1948).

(d) A. E. Seigel, The Rapid Expansion of Compressed Gases behind a Piston, (Doctoral Thesis, University of Amsterdam, January 1952).

(e) NOLM 10819, A Solution of Lagrange's Problem of Interior Ballistics by Means of its Characteristic Lines, by W. H. Heybey.

(f) P. de Haller, Bulletin Tech. Suisse Romande No. 1, 1 (1948) and Schweiz Tech. Rev. No. 1, 6 (1945).

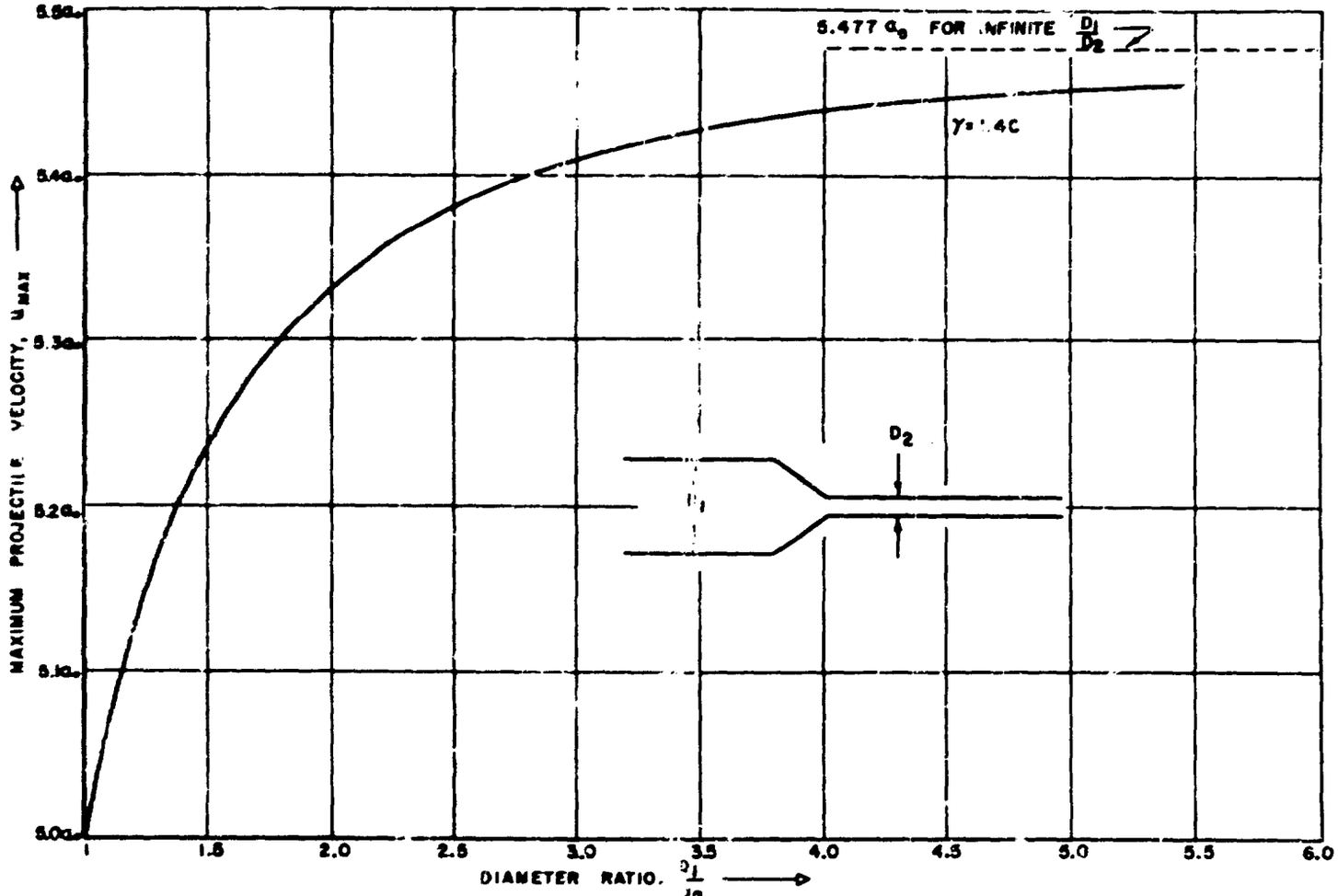

FIG.I THE MAXIMUM PROJECTILE VELOCIT. AS A FUNCTION OF CHAMBER DIAMETER TO BORE DIAMETER FOR AN INF.NITE CHAMBER LENGTH GUN

FIG.I THE MAXIMUM PROJECTILE VELOCITY AS A FUNCTION OF CHAMBER DIAMETER TO

FIG.1 THE MAXIMUM PROJECTILE VELOCITY AS A FUNCTION OF CHAMBER DIAMETER TO BORE DIAMETER FOR AN INFINITE CHAMBER LENGTH GUN

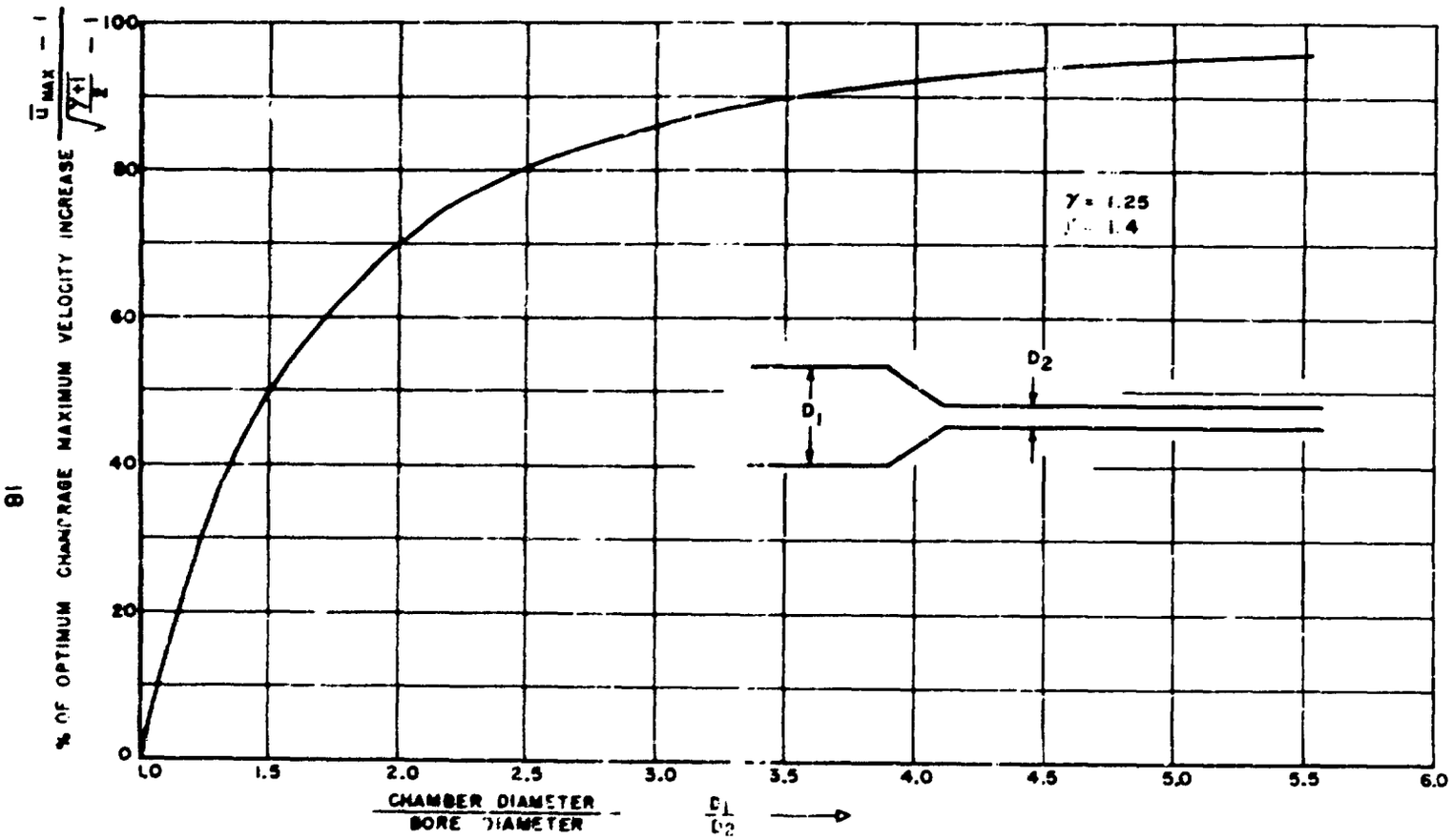

FIG.2 THE PERCENT OF THE OPTIMUM CHAMBRAGE MAXIMUM PROJECTILE VELOCITY INCREASE AS A FUNCTION OF CHAMBER DIAMETER TO BORE DIAMETER FOR AN INFINITE CHAMBER LENGTH GUN

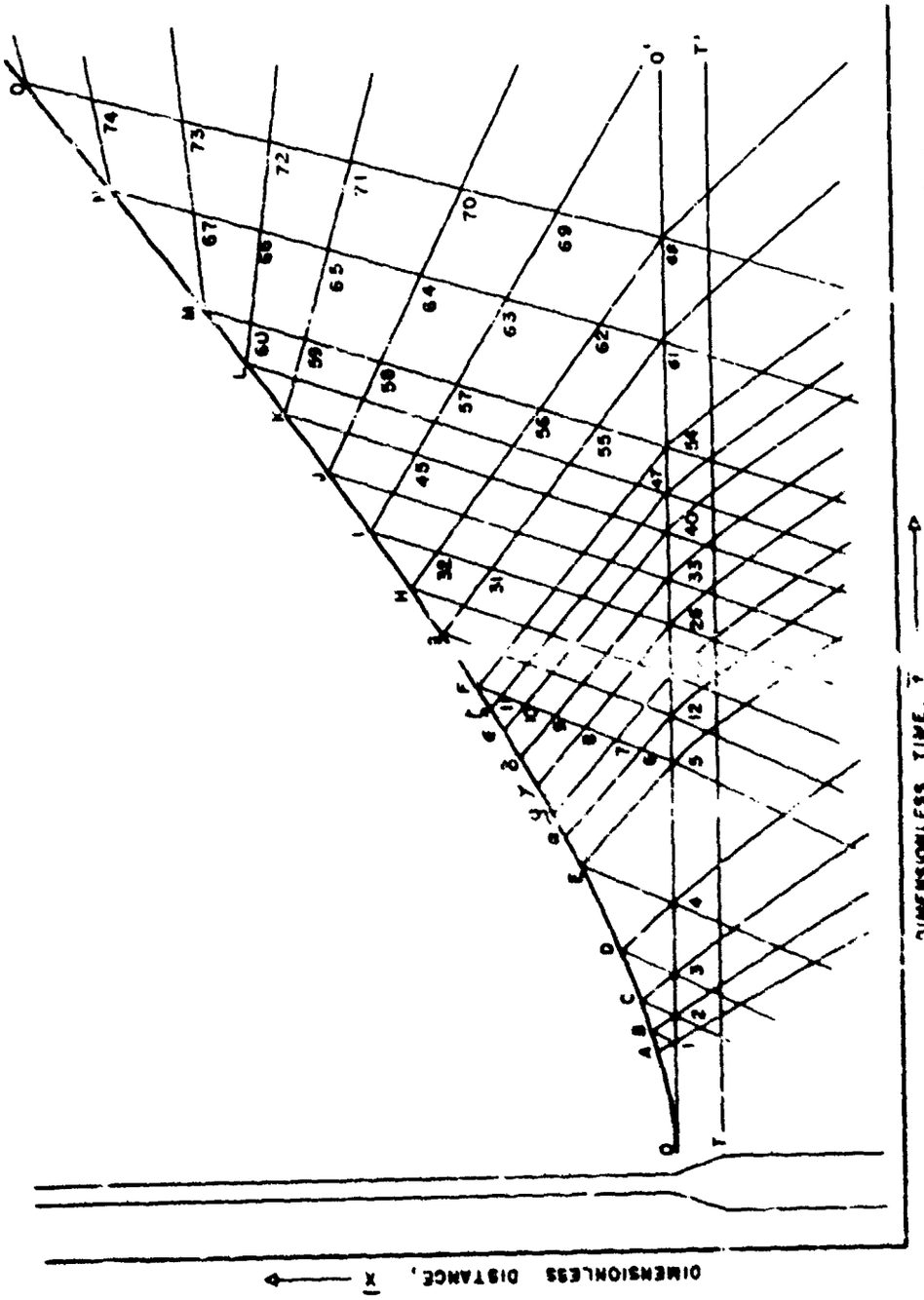

FIG.3 SCHEMATIC CHARACTERISTICS DIAGRAM FOR CHAMBERED GUN

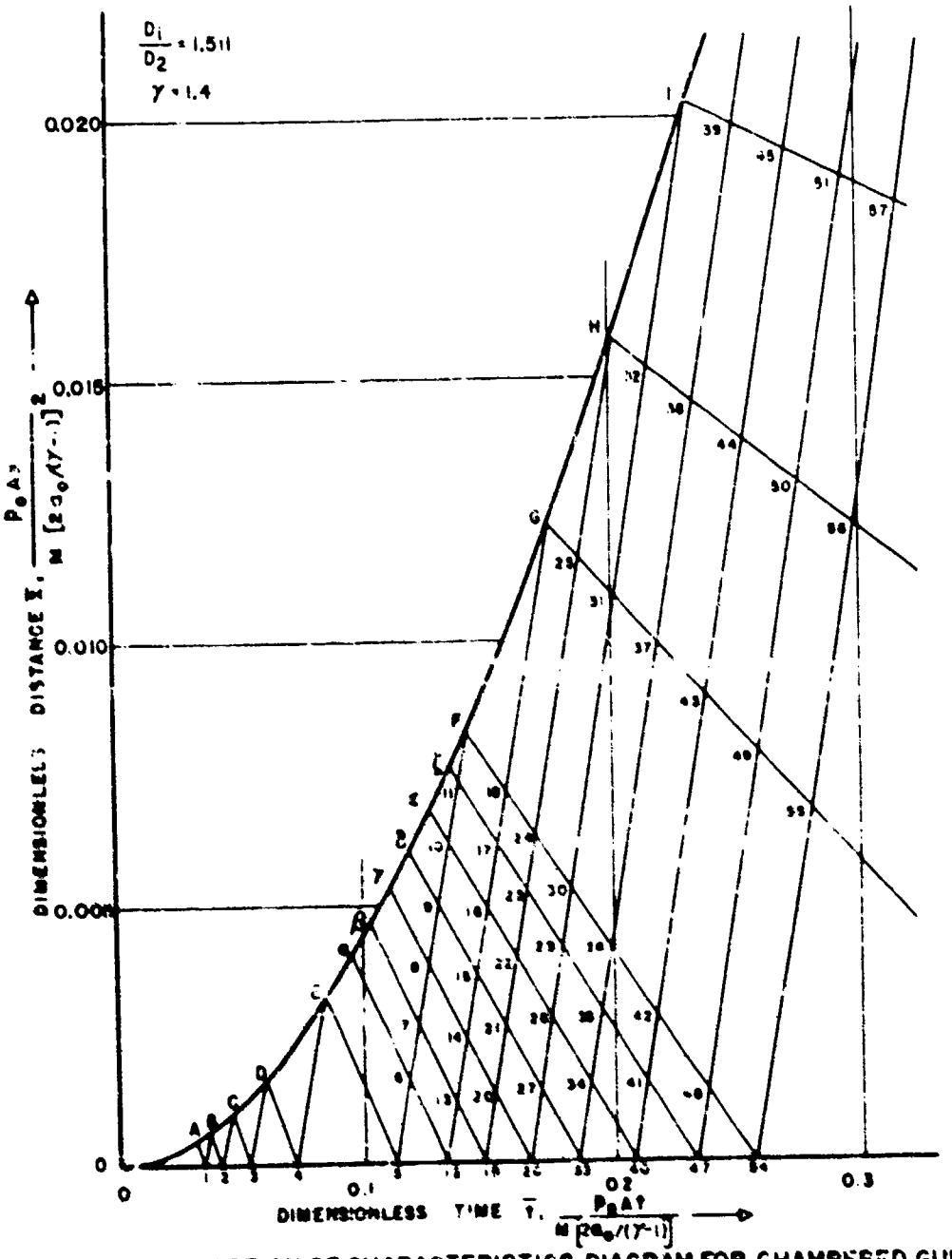

FIG.4 PORTION OF CHARACTERISTICS DIAGRAM FOR CHAMBERED GUN

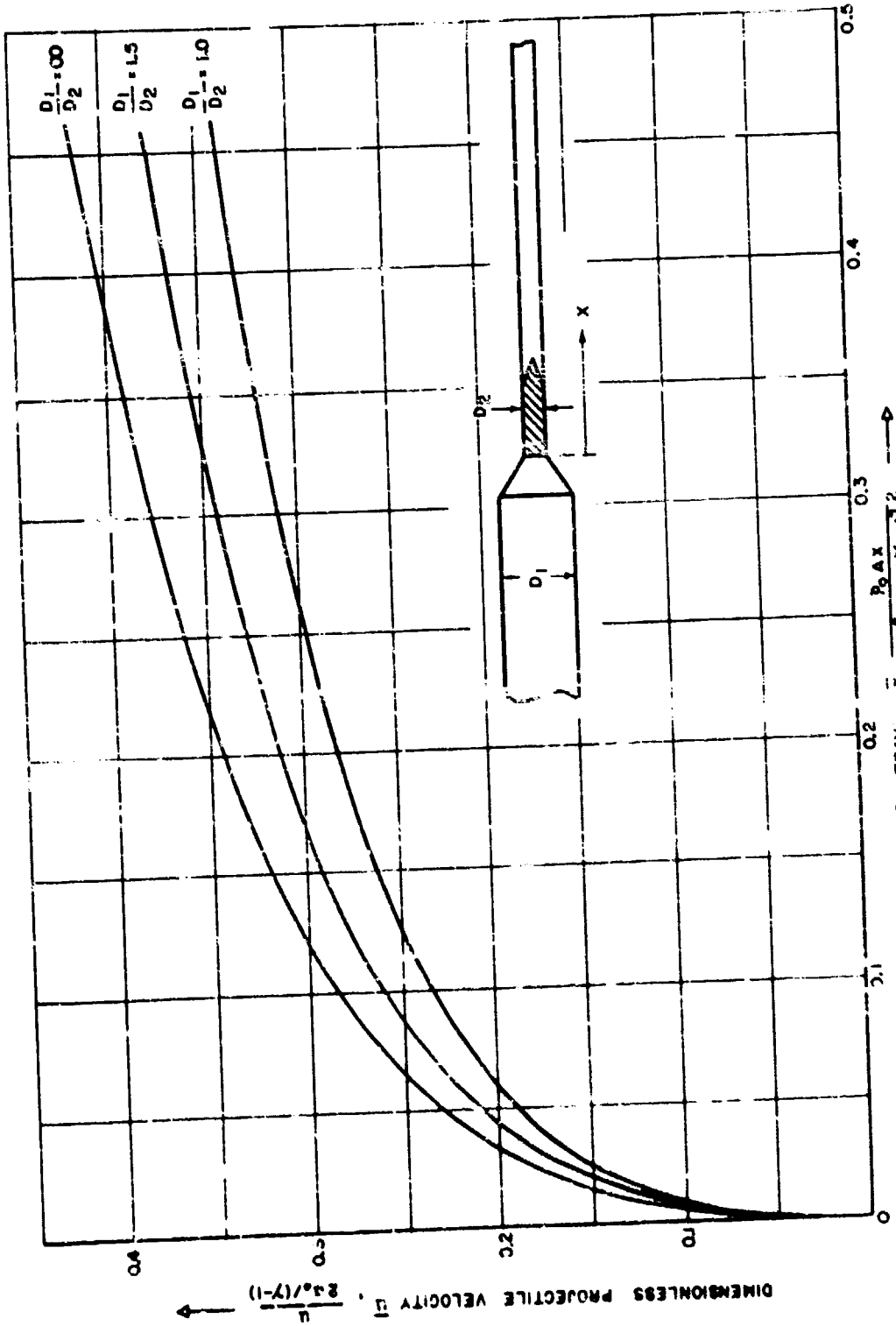

FIG.5 PROJECTILE VELOCITY VS TRAVEL CURVES FOR CHAMBERED GUNS WITH EFFECTIVELY INFINITE LENGTH CHAMBERS FOR γ=1.4

FIG.5 PROJECTILE VELOCITY VS TRAVEL CURVES FOR CHAMBERED GUNS WITH EFFECTIVELY INFINITE LENGTH CHAMBERS FOR γ=1.4

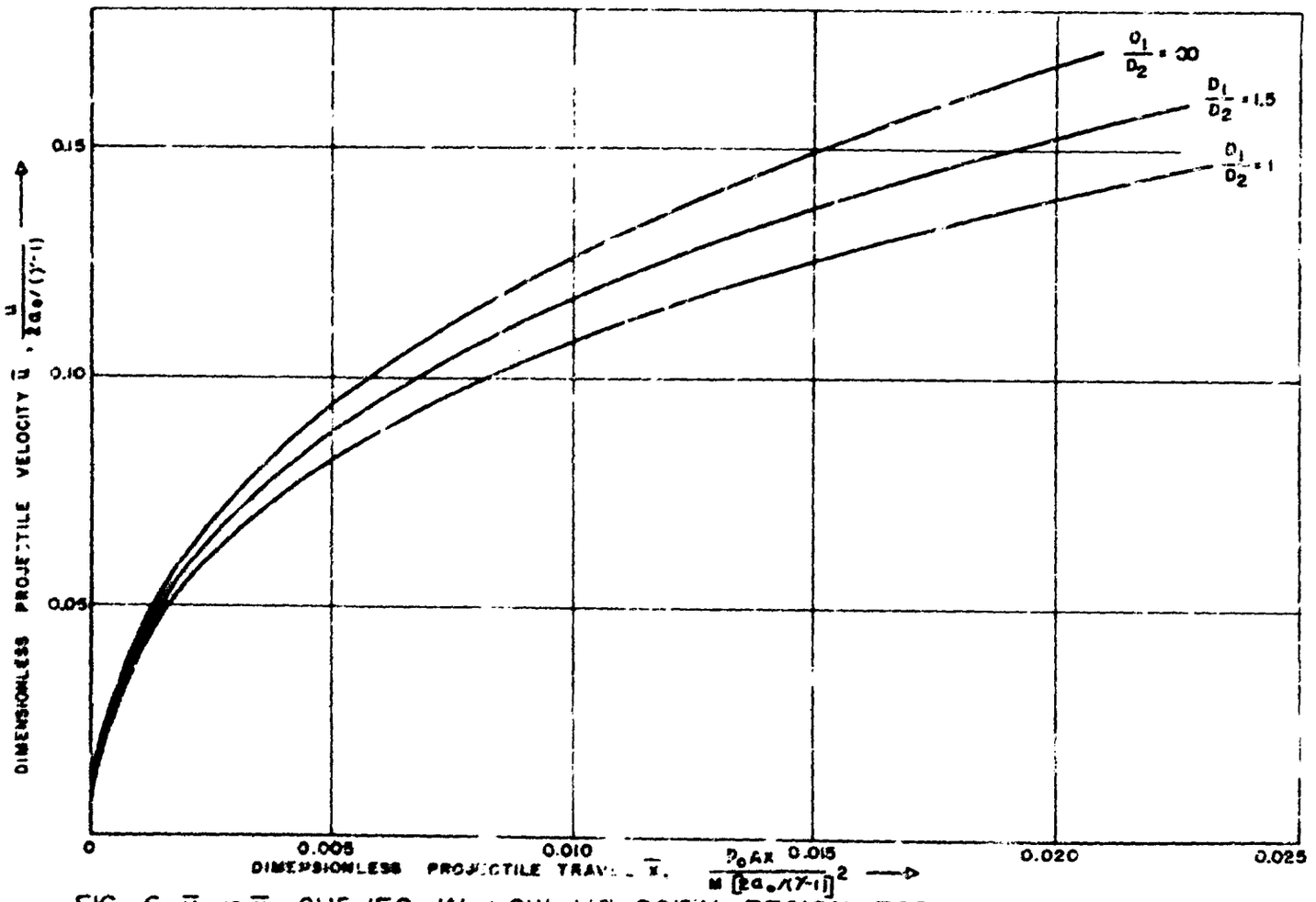

FIG. 6 $\bar{u}$ vs $\bar{x}$ CURVES IN LOW VELOCITY REGION FOR CHAMBERED GUNS WITH EFFECTIVELY INFINITE LENGTH CHAMBERS FOR $\gamma = 1.4$

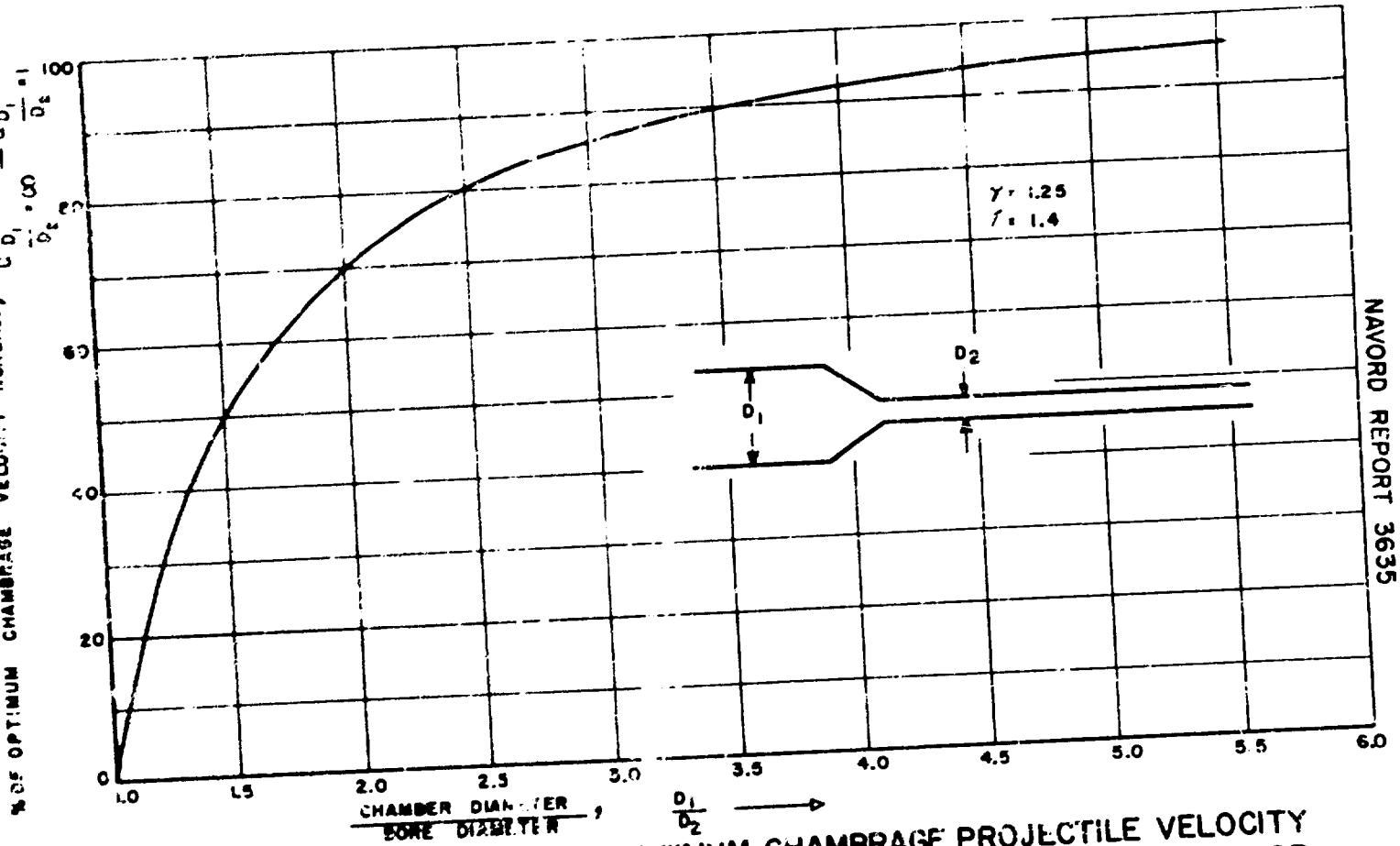

FIG.7 THE PERCENT OF THE OPTIMUM CHAMBRAGE PROJECTILE VELOCITY INCREASE AS A FUNCTION OF CHAMBER DIAMETER TO BORE DIAMETER FOR AN INFINITE CHAMBER LENGTH GUN

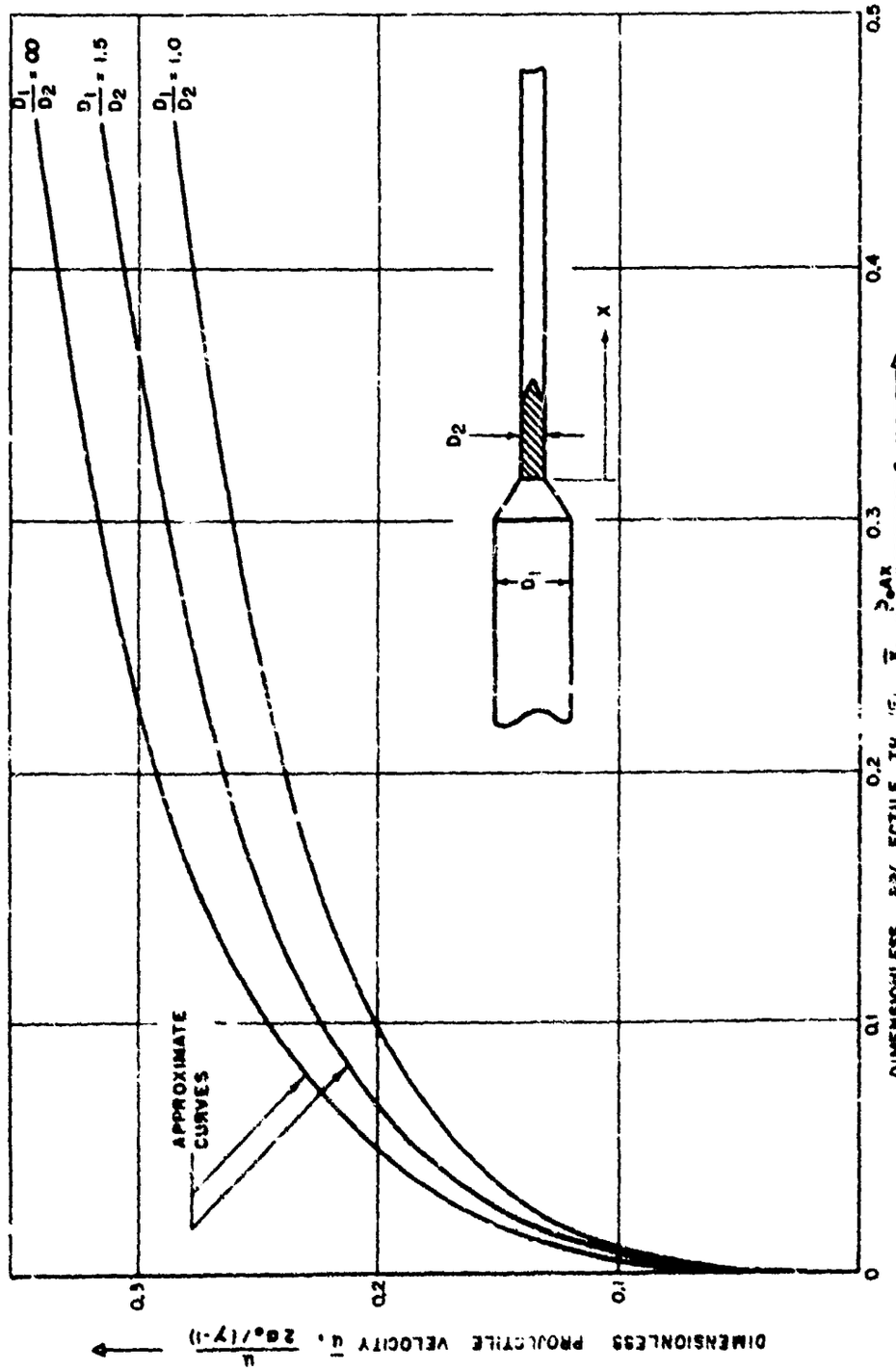

FIG 8 PROJECTILE VELOCITY VS TRAVEL CURVES FOR CHAMBERED GUNS WITH EFFECTIVELY INFINITE LENGTH CHAMBERS FOR $\gamma = 1.25$

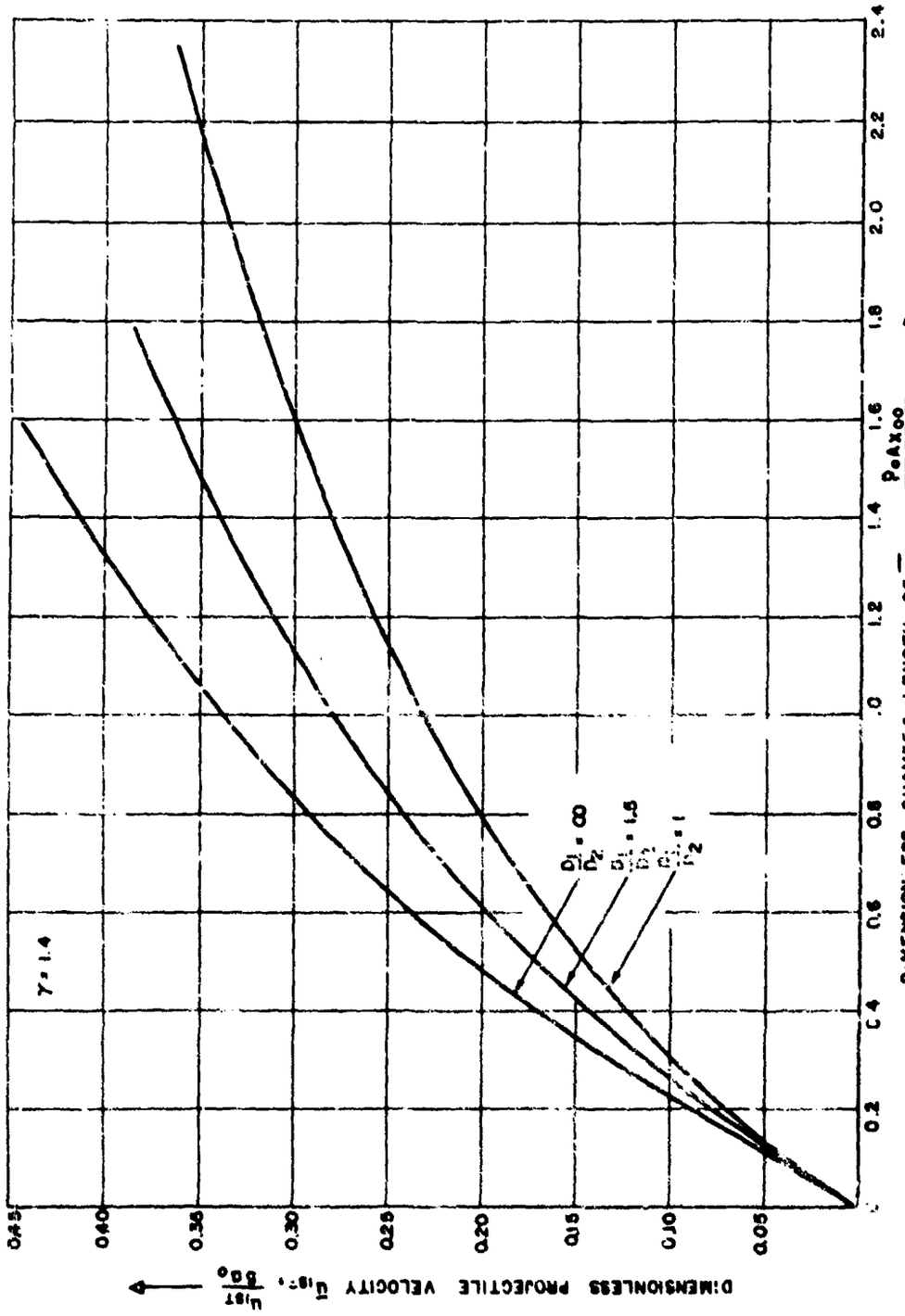

FIG.9 PROJECTILE VELOCITY AS A FUNCTION OF THE LENGTH OF CHAMBER TO BE EFFECTIVELY INFINITE

DIMENSIONLESS CHAMBER LENGTH $25\,x_{00}$, $\frac{MG_c^2}{}$

FIG. PROJECTILE VELOCITY AS A FUNCTION OF THE LENGTH OF CHAMBER

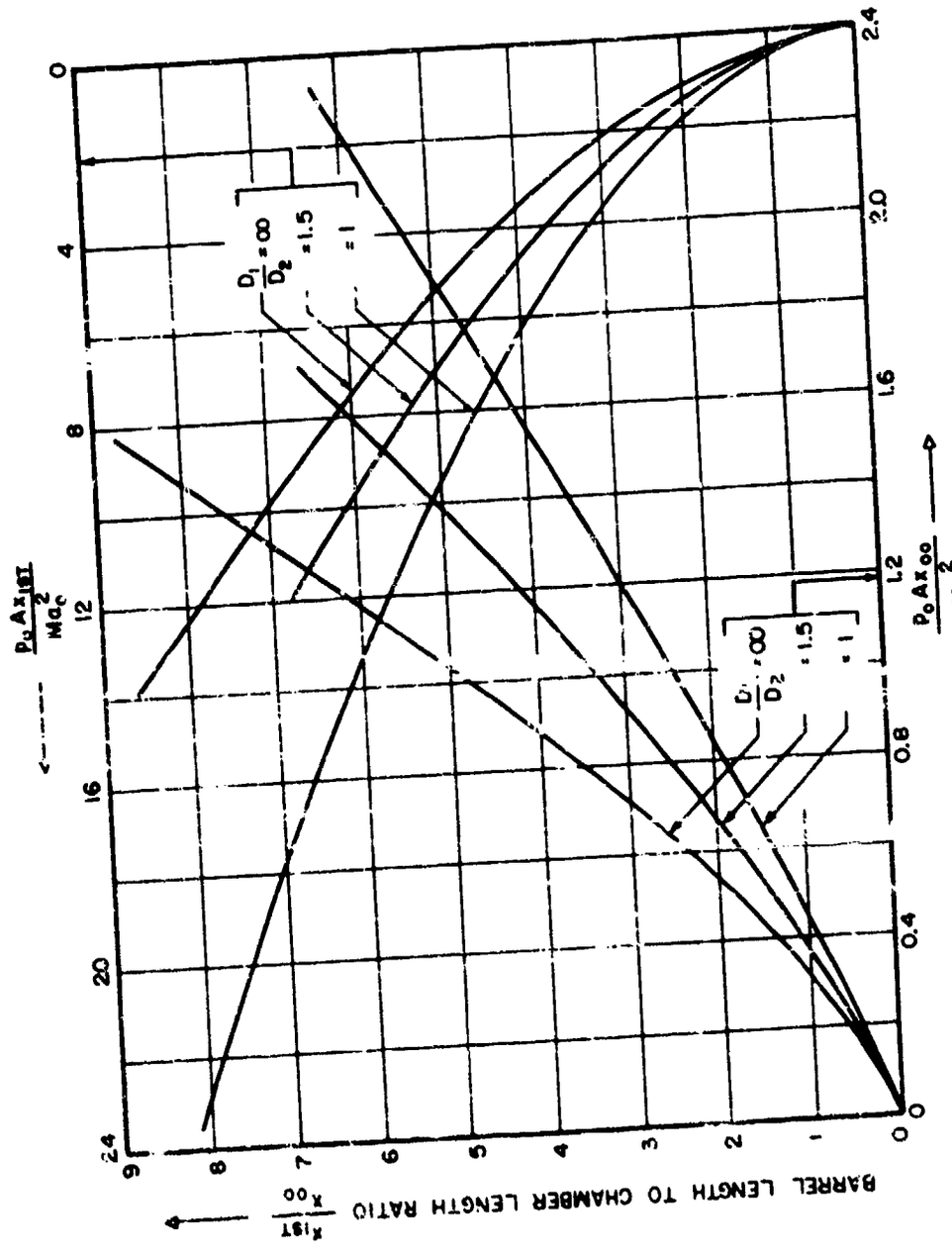

FIG. 10 THE RELATION BETWEEN PROJECTILE TRAVEL AND THE LENGTH OF CHAMBER TO BE EFFECTIVELY INFINITE

FIG.9 PROJECTILE VELOCITY AS A FUNCTION OF THE LENGTH OF CHAMBER TO BE EFFECTIVELY INFINITE

EXTERNAL DISTRIBUTION LIST FOR NAVORD REPORT 3635

	No. of Copies
Department of the Air Force Hq. USAF, DCS/D Washington 25, D. C. Attn: AFDRD-AN, Maj. H. R. Schmidt	1
Commanding General Wright Air Development Center Wright-Patterson Air Force Base, Ohio	
Attn: WCEGH-2	1
Attn: WCLPN-2	1
Attn: WCRRC	1
Commanding General Aberdeen Proving Ground Maryland Attn: Ballistic Research Laboratories ORDBG-BLI	2
Commanding General Frankford Arsenal Bridge and Tacony Streets Philadelphia, Pennsylvania Attn: Pitman-Dunn Laboratory	2
Department of the Army Office, Chief of Ordnance Washington 25, D. C.	
Attn: ORDTA - Propellant and Primer Section	1
Attn: ORDTU	1
Attn: ORDTX-AR	2
Attn: ORDTR	1
Commanding Officer Office of Ordnance Research Box CM Duke Station Durham, North Carolina	3
Commanding Officer Picatinny Arsenal Dover, New Jersey Attn: Library	2
Commanding General Redstone Arsenal Huntsville, Alabama Attn: Technical Library	2

	No. of Copies
Commanding General White Sands Proving Ground Las Cruces, New Mexico Attn: Technical Librarian	3
Department of the Navy Bureau of Aeronautics Washington 25, D. C. Attn: SI-5	1
Department of the Navy Bureau of Ordnance Washington 25, D. C.	
Attn: Ad3, Technical Library	1
Attn: Re2a	1
Attn: Re2d	1
Attn: Re5e	2
	1
Commander U. S. Naval Air Missile Test Center Point Mugu, California Attn: Technical Library	1
Commanding Officer U. S. Naval Air Rocket Test Station Lake Denmark Dover, New Jersey Attn: Technical Library	2
Commanding Officer U. S. Naval Powder Factory Indian Head, Maryland Attn: Research and Development Department	1
Commander U. S. Naval Proving Ground Dahlgren, Virginia Attn: M. I. Division	3
Commander U. S. Naval Ordnance Test Station Inyokern, China Lake, California Attn: Technical Library Branch	1
Department of the Navy Office of Naval Research Washington 25, D. C. Attn: Code 429	1
Commanding Officer Office of Naval Research Branch Office 86 E. Randolph Street Chicago 1, Illinois Attn: LTJG. M. C. Laug	

	No. of Copies
Commanding Officer Office of Naval Research 1030 E. Green Street Pasadena 1, California	1
Department of the Navy Bureau of Aeronautics Washington 25, D. C. Attn: TD-4	1
Aerojet-General Corporation P. O. Box 296 Azusa, California Attn: Librarian via INSMAT	1
Allegany Ballistics Laboratory P. O. Box 210 Cumberland, Maryland via INSMAT	1
Armour Research Foundation of Illinois Institute of Technology Technology Center via INSMAT Chicago 16, Illinois Attn: Propulsion and Structures Research; Department M	1
Atlantic Research Corporation 812 North Fairfax Street Alexandria, Virginia via INSMAT	1
Bureau of Mines 4800 Forbes Street Pittsburgh 13, Pennsylvania Attn: Explosives & Physical Sciences Division	1
E. I. du Pont de Nemours and Company 10th and Market Streets Wilmington, Delaware via INSMAT Attn: W. F. Jackson	1
The Franklin Institute 20th and Parkway via INSMAT Philadelphia 3, Pennsylvania Attn: Chemical Kinetics and Spectroscopy Section, W. E. Scott	1
Goodyear Aircraft Corporation 1210 Massillon Road Akron 15, Ohio via INSMAT Attn: H. E. Sheets	1

	No. of Copies
Hercules Experiment Station Wilmington, Delaware via INSMAT Attn: A. M. Ball	1
Hughes Aircraft Company Florence Avenue at Teale Street Culver City, California via INSMAT Attn: M. C. Beebe	1
Director Jet Propulsion Laboratory 4800 Oak Grove Drive via INSMAT Pasadena 3, California	2
The M. W. Kellogg Company Foot of Danforth Avenue Jersey City, New Jersey via INSMAT Attn: Special Projects Department R. A. Miller	1
Arthur D. Little, Inc. 30 Memorial Drive Cambridge 42, Massachusetts Attn: W. A. Sawyer via INSMAT	1
Arthur D. Little, Inc. 30 Memorial Drive via INSMAT Cambridge 42, Massachusetts Attn: W. C. Lothrop	1
Midwest Research Institute 4049 Pennsylvania Kansas City, Missouri via INSMAT Attn: Technical Director	1
University of Michigan Engineering Research Institute Ann Arbor, Michigan via INSMAT Attn: J. C. Brier	1
Naval Ordnance Research School of Chemistry University of Minnesota via INSMAT Minneapolis 14, Minnesota Attn: B. L. Crawford, Jr.	1
Phillips Petroleum Company Bartlesville, Oklahoma Attn: J. P. Alden via INSMAT	1

	No. of Copies
Purdue University Department of Chemistry Lafayette, Indiana via INSMAT Attn: H. Feuer	1
Rohm and Haas Company Redstone Arsenal Research Division Huntsville, Alabama via INSMAT Attn: Technical Director	1
Solid Propellant Information Agency Applied Physics Laboratory The Johns Hopkins University Silver Spring, Maryland via INSMAT Attn: P. K. Reily, Jr.	9
Standard Oil Company Research Department P. O. Box 431 via INSMAT Whiting, Indiana Attn: W. H. Bahlke	1
Thiokol Chemical Corporation Redstone Arsenal Huntsville, Alabama via INSMAT Attn: Technical Director	2
Thiokol Chemical Corporation 780 N. Clinton Avenue Trenton 7, New Jersey via INSMAT Attn. H. R. Ferguson	1
Thiokol Chemical Corporation Elkton Division via INSMAT Elkton, Maryland Attn: D. W. Kershner	1
U. S. Rubber Company General Laboratories Market and South Streets via INSMAT Passaic, New Jersey Attn: P. O. Tawney	1
Reaction Motors, Inc. Rockaway, New Jersey Attn: Librarian via INSMAT	1
Shell Development Company Emeryville, California via INSMAT Attn: S. S. Sorem	1

	No. of Copies
Phillips Petroleum Company P. O. Box 548 McGregor, Texas via INSMAT Attn: Librarian, J. Wiss	2
University of Arkansas Institute of Science and Technology Fayetteville, Arkansas Attn: M. T. Edmison via INSMAT	1
B. F. Goodrich Company Research Center via INSMAT Brecksville, Ohio Attn: Vice President/Research	1
Universal Match Corporation P. O. Box 191 Ferguson 21, Missouri via INSMAT Attn: Res. and Dev. Division Via: St. Louis Ordnance District	1
British Joint Services Mission Technical Services 1800 K Street, N. W. Washington, D. C. Attn: C. G. Lawson Via: Department of the Navy Bureau of Ordnance Washington 25, D. C. Attn: Ad8	4
Canadian Joint Staff 2001 Connecticut Ave., N. W. Washington 6, D. C. Attn: Defense Research Member Via: Department of the Navy Bureau of Ordnance Washington 25, D. C. Attn: Ad8	4
Catholic University of America 7th St. and Michigan Ave., N. E. Washington 17, D. C. Attn: F. O. Rice via INSMAT	1
Detroit Controls Corporation 806 Chestnut Street Redwood City, California via INSMAT Attn: Research Director Via: Assistant Inspector of Naval Material 533 Middlefield Road Redwood City, California	1

	No. of Copies
Superintendent U. S. Naval Gun Factory Washington 25, D. C.	1
Redel, Incorporated 7405 Varna Street North Hollywood, California Via: Inspector of Naval Material 1206 S. Santee Street Los Angeles 15, California	1
Mathieson Chemical Corporation Research Division Niagara Falls, New York Via: Inspector of Naval Material Hotel Buffalo - 14th Floor Washington and Swan Streets Buffalo 3, New York	1
Experiment, Incorporated P. O. Box 1-T Richmond 2, Virginia Attn: Librarian via INSMAT	1
Navy Research Section Library of Congress c/o Technical Information Division Washington 25, D. C.	1
Office of Naval Research Department of the Navy Washington 25, D. C. Attn: Code 463	1
Cornell Aeronautical Laboratory, Inc. 4455 Genesee Street Buffalo 21, New York Attn: Mr. J. T. Grey via INSMAT	1
Olin Industries, Inc. Winchester Division New Haven, Connecticut Attn: Mr. R. S. Holmes via INSMAT	1
Stanford Research Institute Palo Alto California Attn: Librarian via INSMAT	1

No. of Copies

Hercules Powder Company
Wilmington, Delaware
Attn: Laboratory — via INSMAT — 1

Commanding Officer (R & D) (PC)
Springfield Armory
Springfield, Mass. — 1

Mr. E. H. Smith
E. H. Smith and Company
901 Pershing Drive
Silver Spring, Maryland — via INSMAT — 1

Dr Bernard Lewis
Combustion and Explosives Research, Inc.
Alcoa Building
Pittsburgh 19, Pennsylvania — via INSMAT — 1